SYNTHESIS, STRUCTURAL AND MAGNETIC STUDIES OF COBALT DOPED NICKEL-ZINC FERRITE NANOPARTICLES

SYNOPSIS

Submitted for the partial fulfillment of the requirement for the degree of

DOCTOR OF PHILOSOPHY

IN

PHYSICS AND MATERIALS SCIENCE

BY

RAJINDER KUMAR
Enrollment Number: 136952

Under the supervision of
Prof. P.B. Barman
Dr. Ragini Raj Singh

DEPARTMENT OF PHYSICS AND MATERIALS SCIENCE
JAYPEE UNIVERSITY OF INFORMATION TECHNOLOGY
WAKNAGHAT, SOLAN-173234, INDIA

CONTENTS

1. INTRODUCTION…….....

2. OBJECTIVES OF THE STUDY …….....

2.1. Synthesis, structural and magnetic studies of Co doped Ni-Zn ferrite nanoparticles

2.2 Effect of annealing temperature on structural and magnetic properties of Co doped Ni-Zn ferrite nanoparticles

2.3 Development of Co doped Ni-Zn ferrite nanoparticles by non-aqueous method and their structural and magnetic properties studies

3. REFRENCES …….

4. PUBLICATIONS ……...

1. INTRODUCTION

Now days, soft ferrimagnetic Ni-Zn ferrites are the subject of intense research because they possess high resistivity, moderate saturation magnetization, low coercivity, high Curie temperature, chemical stability and low eddy current losses [1]. Owing to their excellent properties, Ni-Zn ferrites are promising magnetic materials used in many applications such as antenna rods, recording heads, loading coils, core materials for power applications, microwave devices, etc. [2-5]. Ni–Zn ferrite normally has mixed spinel structure which consists of eight tetrahedral (A) and sixteen octahedral (B) sites occupied by the cations. The Zn^{2+} and Fe^{3+} cations are distributed over tetrahedral (A) sites and Ni^{2+} and remaining Fe^{3+} cations are distributed over octahedral (B) sites [6]. The magnetic properties of Ni-Zn ferrites can further be improved by doping [7]. Presently in order to improve the magnetic properties, Co has been introduced in Ni-Zn ferrite system because of its high magnetic moment and positive magneto crystalline anisotropy energy. Among the different reported methods, sol-gel method has been used to prepare the ferrite nanoparticle by virtue of its exclusive advantages such as precursors materials dissolve at atomic or molecular level, low processing temperature, homogeneous reaction distribution, excellent composition control, cost effectiveness and better results over other complex methods. The new method that is non-aqueous method has also been optimized to

prepare the undoped and Co doped Ni-Zn ferrite nanoparticle. Because in non-aqueous method, nanoparticles can be prepared by using non hydrated solvent without using any complexing agent, without adjusting the pH, low temperature synthesis process and in addition very less time is required to prepare the nanoparticles. Moreover, this method is very simple, cost effective and can produce multicomponent nanoparticles system.

2. OBJECTIVES OF THE STUDY

2.1 Objective: Synthesis, structural and magnetic studies of Co doped Ni-Zn ferrite nanoparticles

The highlight of the work is to synthesize and analyze the structural and magnetic properties of undoped and Co doped Ni-Zn ferrite nanoparticles. All the ferrite nanoparticles have been prepared by sol-gel method. Citric acid used as complexing agent which help for the formation of metals cations from precursor materials. Ammonia solution has been used to adjust pH to control the reaction rate. We have employed X-ray diffraction (XRD), field emission scanning electron microscope (FESEM), energy dispersive X-ray spectroscopy (EDX) and vibrating sample magnetometer (VSM) and results are being presented.

Synthesis of $Ni_{0.6-x}Zn_{0.4}Co_xFe_2O_4$ (x = 0, 0.03, 0.033, 0.066, 0.09, 0.132, 0.264, 0.27 and 0.528) nanoparticles: The ferrite nanoparticles have been synthesized by sol gel method. The chemicals nickel nitrate hexahydrate (Ni $(NO_3)_2.6H_2O$), zinc nitrate hexahydrate (Zn $(NO_3)_2.6H_2O$), cobalt nitrate hexahydrate (Co $((NO_3)_2.6H_2O$), ferric nitrate nonahydrate (Fe $(NO_3)_3.9H_2O$) and citric acid monohydrate ($C_6H_8O_7$) were used as raw materials to prepare $Ni_{0.6-x}Zn_{0.4}Co_xFe_2O_4$ nanoparticles. The appropriate amounts of nitrates were dissolved in distilled water under magnetic stirring for 30 minutes then citric acid monohydrate was dissolved in it with a molar ratio of nitrates to citric acid is 1:3. Ammonia solution is added into the solution to adjust pH = 7 kept at 75 ± 5ºC and stirred continuously until the solution changed into gel. The gel was dried at 110 ± 5ºC for 24 hours annealed at 700^0C for five hours. Finally, desired ferrite nanoparticles have been obtained. Schematic diagram of sol-gel method is shown in fig.1. The chemical reaction of prepared nanoparticles is given below:

$$(0.6\text{-}x)Ni(NO_3)_2.6H_2O+(0.4)Zn(NO_3)_2.6H_2O+(x)Co(NO_3)_2.6H_2O+2Fe(NO_3)_3.9H_2O+$$
$$9C_6H_8O_7.H_2O+ NH_3 \xrightarrow{\Delta} Ni_{0.6-x}Zn_{0.4}Co_xFe_2O_4+4N_2\uparrow+54CO_2\uparrow+ 49H_2\uparrow+ 8H_2O$$

where x is doping concentration of Co^{2+} ions.

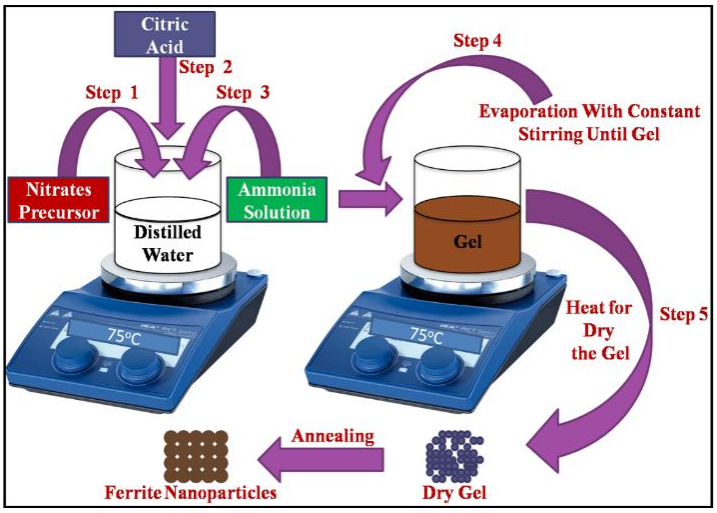

Fig.1: Schematic diagram of sol-gel method.

Structural analysis: The X-ray diffraction spectra of all prepared ferrite nanoparticles have been shown in fig.2. The XRD peaks (111), (022), (113), (222), (004), (224), (333) and (044) indicate that prepared samples at x = 0.264, 0.27 and 0.528 have single phase spinel cubic structure. The other prepared samples at x = 0, 0.03, 0.033, 0.066, 0.09 and 0.132 have partial formation of hematite secondary phase with spinel phase cubic structure. The diffraction peaks have good agreement with standard JCPDS card no. 52-0277 and 89-0599 corresponding to spinel Ni-Zn ferrite and hematite secondary phase respectively. The crystallite size (*D*) (eqn. 1), d-spacing (*d*) (eqn. 2), lattice constant (*a)* (eqn. 3) [8] and strain (ε) (eqn. 4) [9] have been calculated using relation and being presented in table 1:

$$D = k\lambda / \beta\cos\theta \quad \ldots (1), \qquad 2\,d\,\sin\theta = n\,\lambda \quad \ldots (2), \qquad a = d * \sqrt{h^2 + k^2 + l^2} \quad \ldots (3),$$

$$\varepsilon = \beta / 4\tan\theta \quad \ldots (4)$$

where λ is the wavelength of the x-rays used, β the full width at half maximum of prominent (113) XRD peak, and θ the Bragg angle.

It is found that *D* value of prepared nanoparticles first increase at x = 0.03, then decrease at x = 0.033 and further increases with cobalt doping. Also the values of d-spacing (*d*) as well as lattice constant (*a*) first decrease up to x = 0.033 and then increase with Co doping.

Table1. Crystallite size (*D*), d spacing (*d*), lattice constant (*a*) and strain (ε) calculated from the prominent peak (113) of XRD.

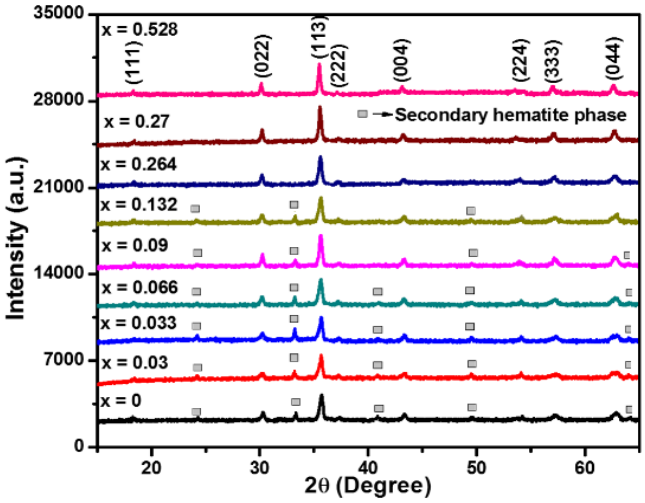

Fig.2: XRD Spectra of $Ni_{0.6-x}Zn_{0.4}Co_xFe_2O_4$ (x = 0, 0.03, 0.033, 0.066, 0.09, 0.132, 0.264, 0.27 and 0.528)

x	*D* (nm)	*d* (Å)	*a* (Å)	ε
0.000	25	2.5209	8.3608	0.00425
0.030	28	2.5195	8.3563	0.00432
0.033	26	2.5143	8.3389	0.00453
0.066	27	2.5161	8.3449	0.00442
0.090	29	2.5173	8.3489	0.00429
0.132	30	2.5191	8.3549	0.00412
0.264	31	2.5205	8.3595	0.00376
0.270	31	2.5209	8.3608	0.00367
0.528	34	2.5267	8.3801	0.00335

Morphology and stoichiometry studies: Fig.3 shows the FESEM micrographs of $Ni_{0.6-x}Zn_{0.4}Co_xFe_2O_4$ at x = 0, 0.03, 0.27 and 0.528. It is observed that the morphology of prepared samples gets changed with Co doping. The stoichiometry study of prepared samples has been performed by EDX. The EDX spectra of $Ni_{0.6-x}Zn_{0.4}Co_xFe_2O_4$ at x = 0, 0.03, 0.264, 0.27 and 0.528 are being presented in fig.4 and atomic compositions are tabulated in table 2. It is found that at x = 0.264, 0.27 and 0.528, all the elements are found in expected composition.

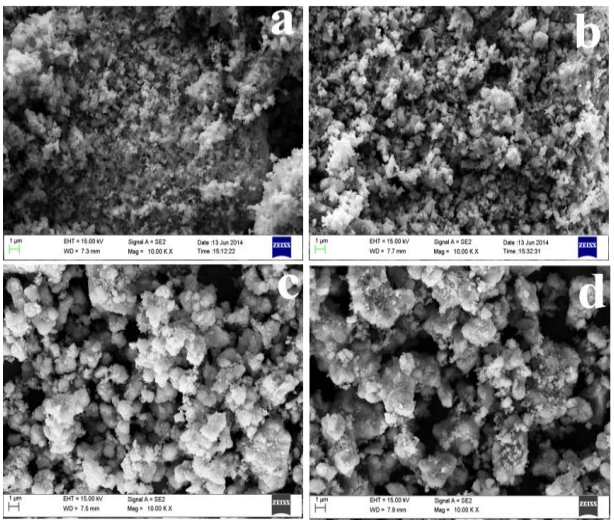

Fig.3: FESEM micrographs of $Ni_{0.6-x}Zn_{0.4}Co_xFe_2O_4$ (a) x = 0, (b) x = 0.03, (c) x = 0.27 and (d) x = 0.528.

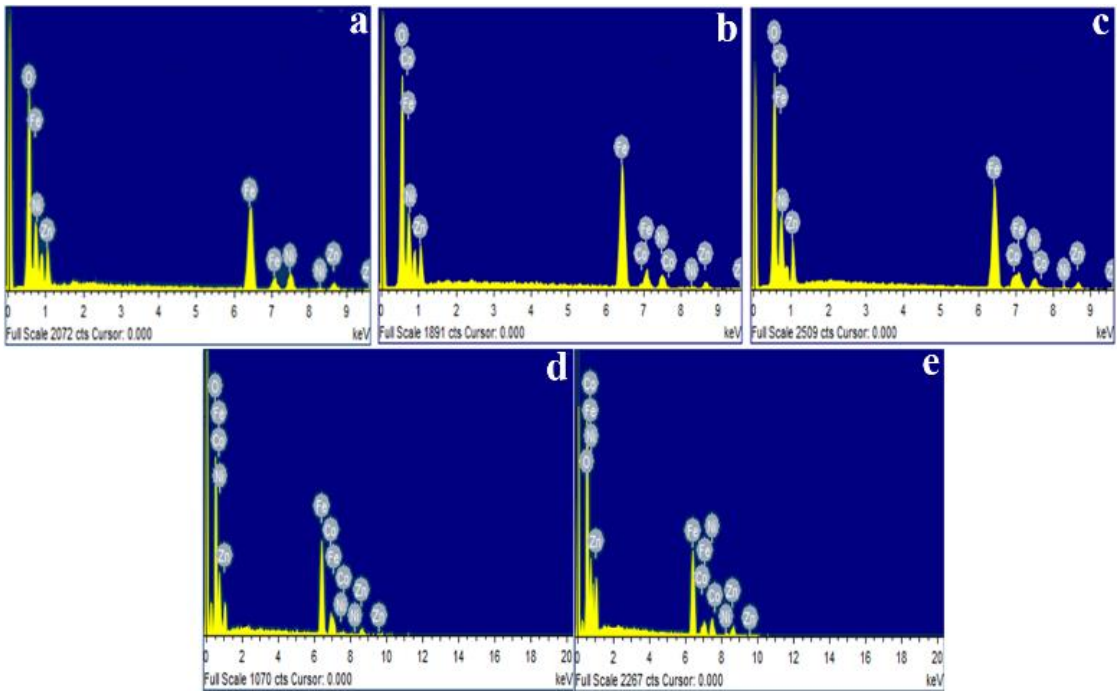

Fig.4: EDX spectra of $Ni_{0.6-x}Zn_{0.4}Co_xFe_2O_4$ (a) x = 0, (b) x = 0.03, (c) x = 0.264, (d) x = 0.27 and (e) x = 0.528.

Table 2. Atomic percentage (At. %) of $Ni_{0.6-x}Zn_{0.4}Co_xFe_2O_4$ at x = 0, 0.03, 0.264, 0.27 and 0.528 obtained from EDX measurement.

Composition (x)	O (At. %)	Fe (At. %)	Ni (At. %)	Zn (At. %)	Co (At. %)
0.000	52.18	33.01	9.98	4.83	0
0.030	50.87	36.41	8.86	3.23	0.63
0.264	57.57	28.97	4.58	5.47	3.41
0.270	56.93	29.12	4.67	5.53	3.75
0.528	57.34	28.89	1.03	5.76	6.98

Magnetic studies: The magnetic properties of $Ni_{0.6-x}Zn_{0.4}Co_xFe_2O_4$ have been studied using VSM at room temperature and M-H curves are illustrated in Fig.5. The obtained values of saturation magnetization (M_s), retentivity (M_r), coercivity (H_c) and squareness ratio (M_r/M_s) are listed in Table 3. Magnetic moment (M_μ) (eqn. 5) [10] and magneto crystalline anisotropy energy (K) (eqn. 6) [11] were calculated and are listed in table 3.

$$M_\mu = (M_w \times M_s)/5585 \quad \text{... (5)} \qquad H_c = 2K/M_s \quad \text{... (6)}$$

where M_w is the molecular weight of the samples.

It is found that M_s first decrease up to x = 0.033 and then increases with Co doping. The value of retentivity (M_r) and coercivity (H_c) have slightly increased with Co doping.

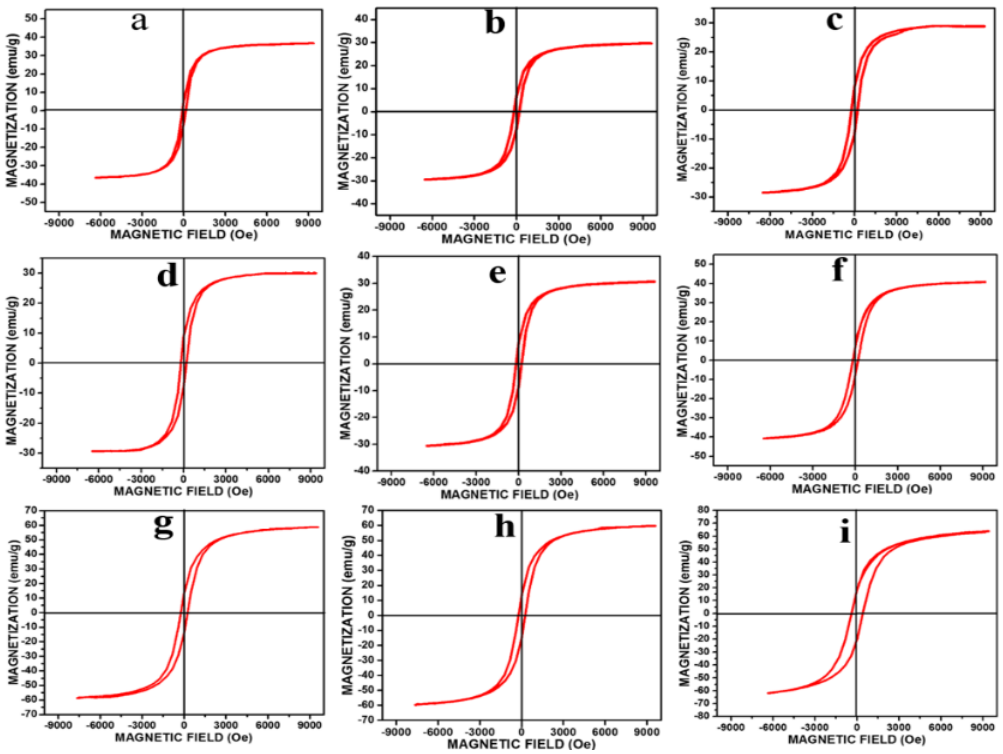

Fig.5: Hysteresis loops of $Ni_{0.6-x}Zn_{0.4}Co_xFe_2O_4$ at (a) x = 0, (b) x = 0.03, (c) x = 0.033, (d) x = 0.066, (e) x = 0.09, (f) x = 0.132, (g) x = 0.264, (h) x = 0.27 and (i) x = 0.528 at room temperature (300K).

Table 3. Saturation magnetization (M_s), magnetic moment (M_μ), retentivity (M_r), coercivity (H_c), squareness ratio (M_r/M_s) and magneto crystalline anisotropy (K) measured using VSM.

***x* (Co Doping)**	***M*$_s$ (emu/g)**	***M*$_\mu$ (μ_B)**	***M*$_r$ (emu/g)**	***H*$_c$ (Oe)**	***M*$_r$/*M*$_s$**	***K* (erg/cm^3)**
0.000	35.61	1.511	06.24	126.28	0.1752	2248.41
0.030	29.58	1.255	07.15	188.00	0.2417	2780.52
0.033	27.63	1.172	07.65	189.32	0.2768	2615.45
0.066	29.73	1.262	08.32	191.73	0.2807	2850.06
0.090	30.57	1.297	08.98	193.11	0.2937	2951.68
0.132	40.95	1.738	10.12	202.25	0.2471	4141.06
0.264	58.53	2.485	13.95	234.45	0.2383	6861.17
0.270	59.75	2.536	14.26	236.46	0.2386	7064.24
0.528	63.25	2.686	18.43	448.23	0.2913	14175.27

Theoretical analysis: The confirmation of variation in structural and magnetic properties with Co doping has been done theoretically from most suitable proposed cations distribution.

Structural and magnetic analysis: The theoretical lattice constant (a_{th}) (eqn.7), mean ionic radii of site A (r_A) (eqn.8), B (r_B) (eqn.9) [12] and theoretical magnetic moments (N_μ) (eqn. 10) [13] were calculated from proposed cations distribution and tabulated in table 4.

$$a_{th} = 8/3\sqrt{3}[(r_A + R_o) + \sqrt{3}(r_B + R_o)] \quad \ldots (7)$$

$$r_A = [C_{Zn2+}.r_{Zn2+} + C_{Fe3+}.r_{Fe3+}] \ldots (8)$$

$$r_B = 1/2[C_{Ni2+}.r_{Ni2+} + C_{Co2+}.r_{Co2+} + C_{Fe3+}.r_{Fe3+}] \quad \ldots (9)$$

$$N_\mu = M(B) - M(A) \quad \ldots (10)$$

Where R_o is the ionic radii of oxygen 1.32 Å. *C* and *r* are the concentration and ionic radii of cations respectively. *M(B)* and *M(A)* are the magnetic moments of B and A sites respectively.

Table 4. Proposed cations distribution, mean ionic radii of tetrahedral site (r_A), mean ionic radii of octahedral site (r_B), theoretical lattice constant (a_{th}), experimental lattice constant (a) and magnetic moment (N_μ).

x	***Cation Distribution Site A***	***Cation Distribution Site B***	r_A **(Å)**	r_B **(Å)**	a_{th} **(Å)**	***a* (Å)**	N_μ **(μ_B)**
0.000	$(Zn_{0.4}Fe_{0.6})$	$[Ni_{0.6}Fe_{1.4}]$	0.7300	0.6760	8.4786	8.3608	5.200
0.030	$(Zn_{0.4}Fe_{0.6})$	$[Ni_{0.57}Co_{0.03}Fe_{1.4}]$	0.7300	0.6768	8.4808	8.3563	5.230
0.033	$(Zn_{0.4}Fe_{0.6})$	$[Ni_{0.567}Co_{0.033}Fe_{1.4}]$	0.7300	0.6769	8.4810	8.3389	5.233
0.066	$(Zn_{0.4}Fe_{0.6})$	$[Ni_{0.534}Co_{0.066}Fe_{1.4}]$	0.7300	0.6778	8.4834	8.3449	5.266
0.090	$(Zn_{0.4}Fe_{0.6})$	$[Ni_{0.51}Co_{0.09}Fe_{1.4}]$	0.7300	0.6784	8.4850	8.3489	5.290
0.132	$(Zn_{0.4}Fe_{0.6})$	$[Ni_{0.468}Co_{0.132}Fe_{1.4}]$	0.7300	0.6796	8.4882	8.3549	5.332
0.264	$(Zn_{0.4}Fe_{0.6})$	$[Ni_{0.336}Co_{0.264}Fe_{1.4}]$	0.7300	0.6832	8.4978	8.3595	5.464
0.270	$(Zn_{0.4}Fe_{0.6})$	$[Ni_{0.33}Co_{0.27}Fe_{1.4}]$	0.7300	0.6834	8.4984	8.3608	5.470
0.528	$(Zn_{0.4}Fe_{0.6})$	$[Ni_{0.072}Co_{0.528}Fe_{1.4}]$	0.7300	0.6905	8.5173	8.3801	5.728

The theoretical a_{th} and N_μ values are found to continuously increasing with Co doping. The variation in a_{th} from *a* and N_μ from M_μ values are due to non-consideration of hematite secondary phase effect in theoretical calculation. Finally, to conclude; a_{th} and N_μ have good agreement with experimental results and support the proposed cations distribution.

2.2 Objective: Effect of annealing temperature on structural and magnetic properties of Co doped Ni-Zn ferrite nanoparticles

In objective 2.1, $Ni_{0.6-x}Zn_{0.4}Co_xFe_2O_4$ nanoparticles have been synthesized by sol-gel method annealed at 700°C. It is found that the prepared nanoparticles with variations of Co doping at x = 0, 0.033, 0.066, 0.132, 0.264, 0.528 has reached to maximum replacement of Ni ions and attain high saturation magnetization than prepared nanopaticles with variation (x = 0, 0.03, 0.09, 0.27). It is also seen that the variation in structural and magnetic properties from x = 0.033 to 0.264 of Co doping are very small. Therefore, composition x = 0.03, 0.066, 0.09, 0.132 and 0.27 are not considered in present study. In order to improve the magnetic properties of nanoparticles and to remove the impurity phase, $Ni_{0.6-x}Zn_{0.4}Co_xFe_2O_4$ (x = 0, 0.0165, 0.033, 0.264 and 0.528) has

been synthesized by sol–gel method and annealed at high temperature 1100°C. The synthesis parameters of objective 2.2 is same as followed in objective 2.1 with only high annealing temperature (1100°C).

Structural analysis: The XRD patterns are presented in fig.6. The calculated values of *D*, *d*, *a* and ε [8-9] are tabulated in table 5. The XRD peaks at (111), (022), (113), (222), (004), (224), (333) and (044) indicates that the prepared samples at x = 0, 0.033, 0.264 and 0.528 have single phase spinel cubic structure. It is found that when samples annealed at 1100°C, hematite phase diminished other than at x = 0.0165. Also the crystallite size (*D*) of samples annealed at 1100°C is slightly smaller than that of samples annealed at 700°C. The calculated values of *d* and *a* initially decreases from x = 0.0165 to 0.033 and then increases with Co doping. The value of ε first increase at x = 0.0165 and then decrease with Co doping.

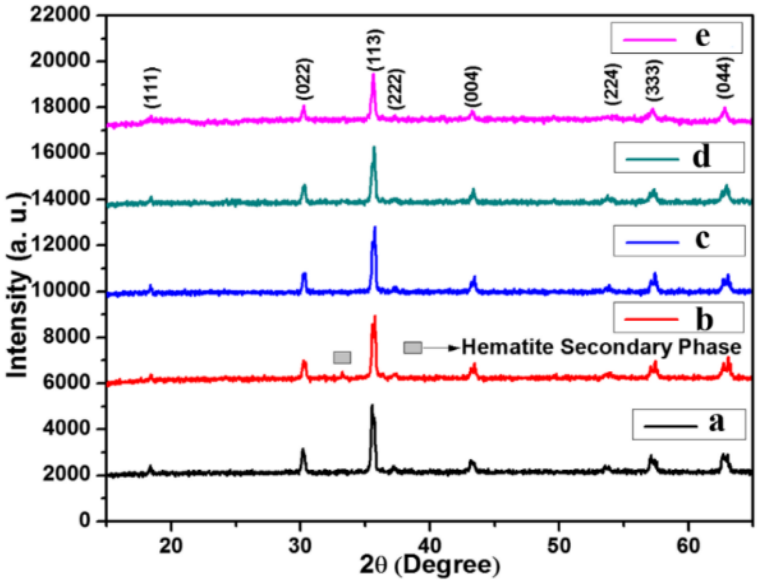

Fig.6: XRD Spectra of (a (x = 0), b (x = 0.0165), c (x = 0.033, d (x = 0.264) and e (x = 0.528)).

Table 5. Crystallite size (*D*), d-spacing (*d*), lattice constant (*a*) and strain (ε).

***x* (Co doping)**	***D* (nm)**	***d* (Å)**	***a* (Å)**	**ε**
0.000	23.59	2.5218	8.3638	0.00480
0.0165	20.21	2.5174	8.3492	0.00508
0.033	22.89	2.5171	8.3451	0.00494
0.264	23.25	2.5193	8.3523	0.00486
0.528	27.37	2.5204	8.3560	0.00413

Morphology and stoichiometry studies: Fig.7 shows the FESEM micrographs of $Ni_{0.6-x}Zn_{0.4}Co_xFe_2O_4$. Morphology of samples annealed at 1100^{o}C is different form that samples when annealed at 700^{o}C (objective 2.1). It is clearly seen in FESEM micrograph, samples annealed at 1100^{o}C are highly crystalline in nature than samples annealed at 700^{o}C. Moreover, crystallinity also improves with annealing temperature [14].

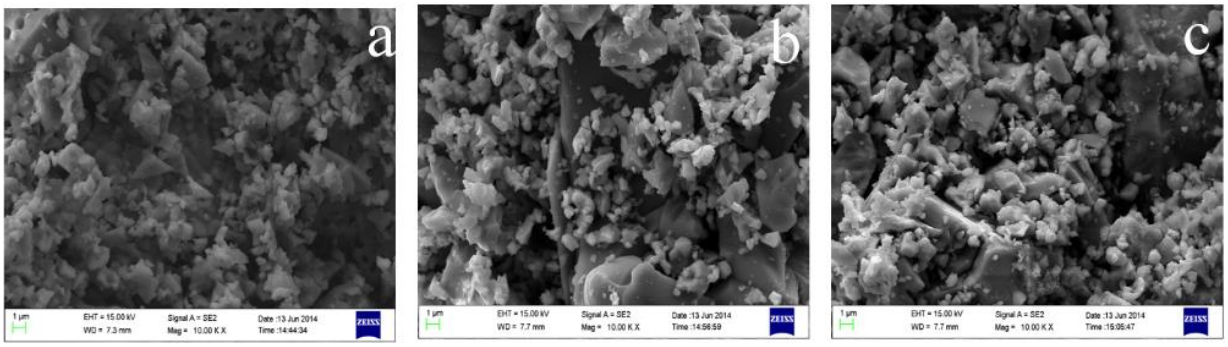

Fig.7: FESEM Micrographs of $Ni_{0.6-x}Zn_{0.4}Co_xFe_2O_4$ (a) x = 0, (b) x = 0.033 and (c) x = 0.264

EDX spectra of the samples are shown in fig.8. The atomic compositions of the samples are tabulated in table 6, which reveals that prepared samples annealed at 1100^{o}C other than at x = 0.0165, all elements are present in definite and expected ratio. As seen in objective 2.1, samples annealed at 700^{o}C are maximum in off-stoichiometry which become stoichiometric when annealed at 1100^{o}C. As at high annealing temperatures impurity phase diminishes.

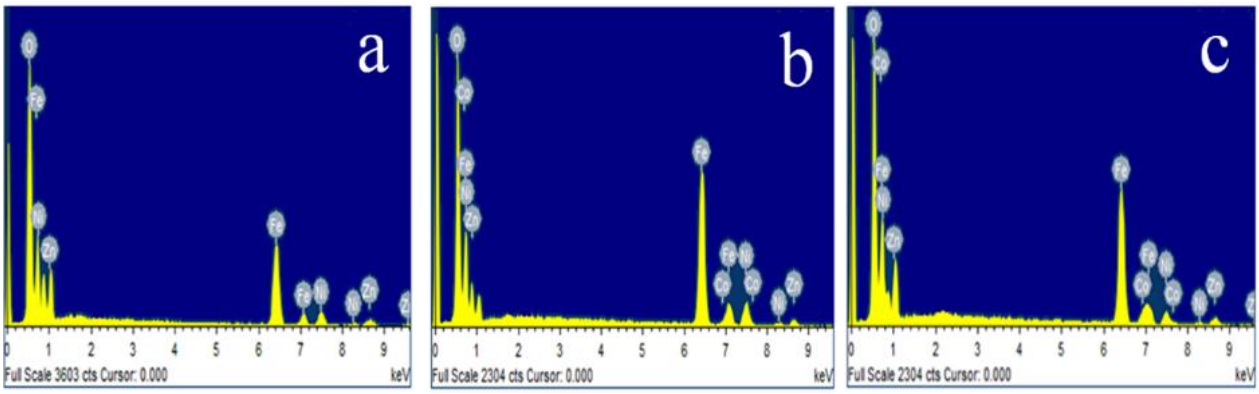

Fig.8: EDX spectra of $Ni_{0.6-x}Zn_{0.4}Co_xFe_2O_4$ (a) x = 0, (b) x = 0.033 and (c) x = 0.264.

Table 6. Atomic percentage (At. %) of $Ni_{0.6-x}Zn_{0.4}Co_xFe_2O_4$ at x = 0, 0.033 and 0.264 obtained from EDX measurement.

Composition (x)	O (At. %)	Fe (At. %)	Ni (At. %)	Zn (At. %)	Co (At. %)
0	55.62	28.70	8.97	6.71	0
0.033	58.12	29.13	6.80	5.69	0.26
0.264	55.29	30.05	4.37	6.67	3.62

Magnetic analysis: The M-H curve of prepared nanoparticles are presented in fig.9. The obtained values of M_s, M_μ, M_r, H_c, M_r/M_s and K from VSM are listed in table 7.

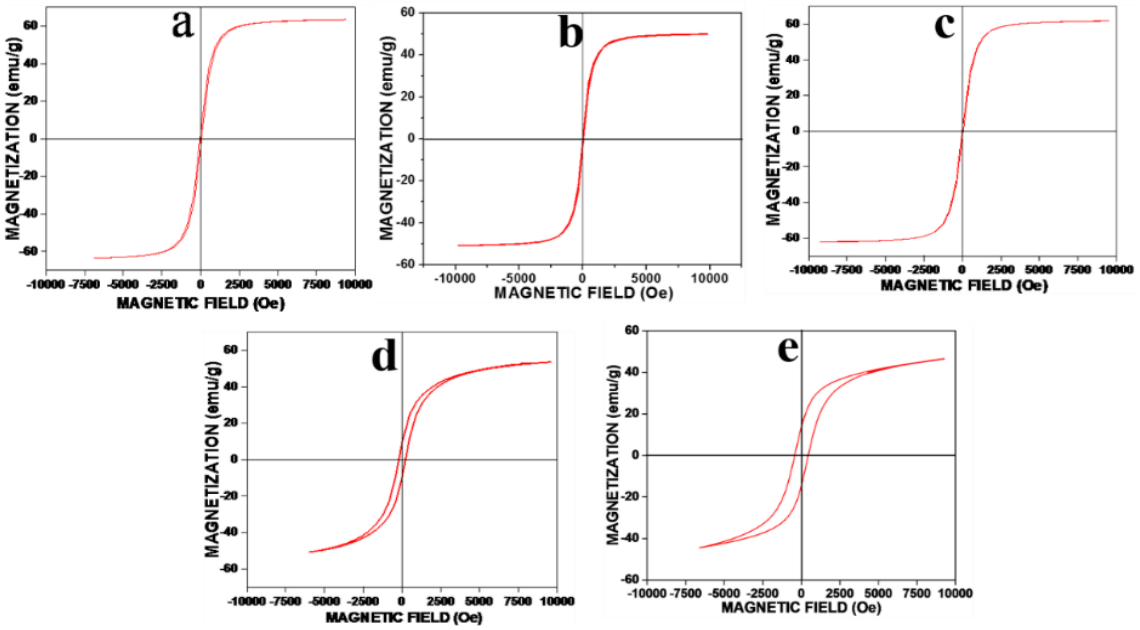

Fig.9: Hysteresis loops of $Ni_{0.6-x}Zn_{0.4}Co_xFe_2O_4$ (a) x = 0, (b) x = 0.0165, (c) x = 0.033, (d) x = 0.264 and (e) x = 0.528 at room temperature (300K).

Table 7. Saturation magnetization (M_s), magnetic moment (M_μ), retentivity (M_r), coercivity (H_c), squareness ratio (M_r/M_s) and magneto crystalline anisotropy (K) measured from VSM.

***x*(Co doping)**	***D* (nm)**	***M*$_s$ (emu/g)**	***M*$_\mu$ (μ_B)**	***M*$_r$ (emu/g)**	***H*$_c$ (Oe)**	***M*$_r$/*M*$_s$**	***K* (erg/cm^3)**
0.000	23.59	63.52	2.696	3.68	49.94	0.058	1586
0.0165	20.21	50.49	2.143	2.61	45.63	0.051	1151
0.033	22.89	61.97	2.630	2.54	35.98	0.041	1115
0.264	23.25	51.95	2.205	9.56	215.92	0.184	5609
0.528	27.37	45.46	1.930	14.14	436.79	0.311	9930

The value of M_s at x = 0 is higher when annealed at 1100^{o}C then sample annealed at 700^{o}C, since the cations distribution is same at both temperatures. Further, with doping M_s continuously decrease. The value of M_r and H_c initially decreases up to x = 0.033 with respect to x = 0 and then increases with Co doping. The obtained value of M_r, H_c and K at 1100^{o}C annealed samples is lower than that obtained when samples annealed at 700^{o}C (objective 2.1).

Theoretical structural and magnetic analysis: The proposed cations distribution, theoretically calculated lattice constant (a_{th}), mean ionic radii of tetrahedral (r_A) and octahedral (r_B) sites [12] and magnetic moment (N_μ) [13] are listed in table 8.

Table 8. Proposed Cations distribution, r_A, r_B, a_{th}, a and N_μ.

x	Cation Distribution Site A	Cation Distribution Site B	r_A (Å)	r_B (Å)	a_{th} (Å)	a (Å)	N_μ
0.0000	$(Zn_{0.4}Fe_{0.6})$	$[Ni_{0.6}Fe_{1.4}]$	0.730	0.676	8.4786	8.3608	5.200
0.0165	$(Co_{0.0165}Zn_{0.3835}Fe_{0.6})$	$[Zn_{0.0165}Ni_{0.5835}Fe_{1.4}]$	0.728	0.677	8.4782	8.3492	5.117
0.0330	$(Co_{0.033}Zn_{0.367}Fe_{0.6})$	$[Zn_{0.033}Ni_{0.567}Fe_{1.4}]$	0.726	0.678	8.4778	8.3451	5.035
0.2640	$(Co_{0.176}Zn_{0.224}Fe_{0.6})$	$[Zn_{0.176}Co_{0.088}Ni_{0.336}Fe_{1.4}]$	0.716	0.689	8.4917	8.3523	4.408
0.5280	$(Co_{0.352}Zn_{0.048}Fe_{0.6})$	$[Zn_{0.352}Co_{0.176}Ni_{0.072}Fe_{1.4}]$	0.703	0.707	8.5197	8.3560	3.616

The calculated theoretically a_{th} and N_μ follow the same trend as calculated a and M_μ from experimental XRD data respectively. Finally, to concluded, the calculated theoretical results have great agreement with the results obtained experimentally and support the proposed cations distributions.

2.3 Objective: Development of Co doped Ni-Zn ferrite nanoparticles by non-aqueous method and their structural and magnetic studies

In the present study, new method i.e. non-aqueous method has been optimized to prepare the $Ni_{0.6-x}Zn_{0.4}Co_xFe_2O_4$ nanoparticles. The nanoparticles prepared by non-aqueous method are highly crystalline in nature, have high saturation magnetization and low value of coercivity as compared to previous synthesized samples by sol-gel method and these materials can be useful in target drug delivery, hyperthermia, EMI shielding and magnetic recording devices applications.

Synthesis of $Ni_{0.6-x}Zn_{0.4}Co_xFe_2O_4$ (x = 0, 0.033, 0.066, 0.132, 0.264 and 0.528) nanoparticles:
Nanoparticles of $Ni_{0.6-x}Zn_{0.4}Co_xFe_2O_4$ (x = 0, 0.033, 0.066, 0.132, 0.264 and 0.528) have been prepared by new method that is non aqueous method. Nickel nitrate hexahydrate (Ni $(NO_3)_2.6H_2O$), zinc nitrate hexahydrate (Zn $(NO_3)_2.6H_2O$), cobalt nitrate hexahydrate (Co $((NO_3)_2.6H_2O$) and ferric nitrate nonahydrate (Fe $(NO_3)_3.9H_2O$) were used as precursor materials to prepare the nanoparticles. Acetone was used as a solvent. The appropriate amounts of Nickel nitrate hexahydrate (Ni $(NO_3)_2.6H_2O$), zinc nitrate hexahydrate (Zn $(NO_3)_2.6H_2O$), cobalt nitrate hexahydrate (Co $((NO_3)_2.6H_2O$) and ferric nitrate nonahydrate (Fe $(NO_3)_3.9H_2O$) have been dissolved in acetone under magnetic stirring for 30 minutes. The reaction was performed at 50 ± 5^oC with continuous stirring until the solution changed into paste. Finally, prepared paste was annealed at 1100^oC for five hours and desired product $Ni_{0.6-x}Zn_{0.4}Co_xFe_2O_4$ nanoparticles have

been formed. Schematic diagram of non-aqueous method is shown in fig.10. The chemical reaction of non-aqueous method is given below:

$$(0.6-x)Ni(NO_3)_2.6H_2O + (0.4)Zn(NO_3)_2.6H_2O + (x)Co(NO_3)_2.6H_2O + 2Fe(NO_3)_3.9H_2O + (CH_3)_2CO$$
$$\underset{\Delta}{\Rightarrow} Ni_{0.6-x}Zn_{0.4}Co_xFe_2O_4 + 2N_2\uparrow + CO_2\uparrow + H_2\uparrow + 6O_2\uparrow + 23H_2O + 4NO_2 + 2CH_3OH$$

where x is doping concentration of Co^{2+} ions.

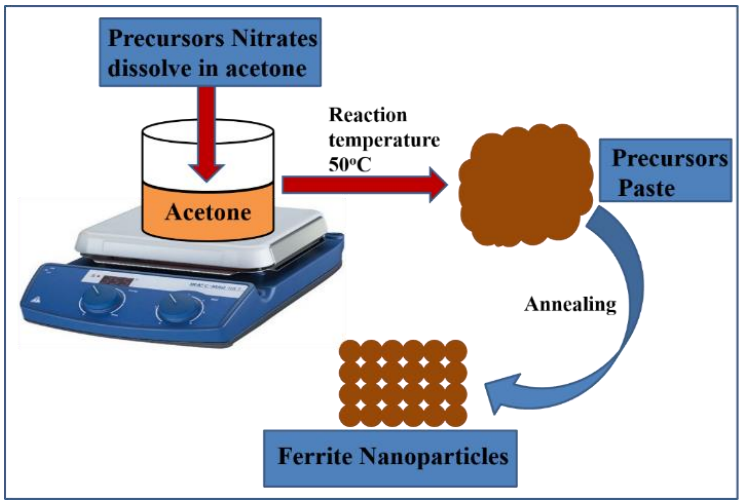

Fig.10: Schematic diagram of non-aqueous method.

Structural analysis: XRD spectra of prepared samples are shown in fig.11 and all the indexed peaks point to the formation of single phase spinel cubic structure. There is no evidence of any other impurity phase in the XRD spectra. The sharp peaks in XRD spectra shows that prepared samples by non-aqueous method are highly crystalline in nature.

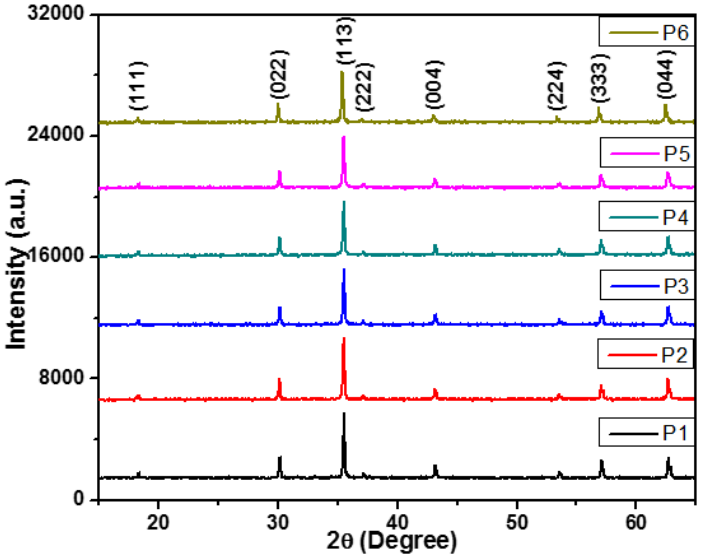

Fig.11: XRD Spectra (P1 (x = 0), P2 (x = 0.033, P3 (x = 0.066), P4 (x = 0.132), P5 (x = 0.264) and P6 (x = 0.528)).

The *D*, *d*, *a* and ε values has been calculated [8-9] and tabulated in table 9. The *D* values of samples prepared by non-aqueous method are found in the range of 51.61 to 59.39 nm with Co doping. The *D* value of prepared nanoparticles are larger than the nanopaticles prepared by sol-gel method (Objective 2.2). The *D*, *d* and *a* values first increase at x = 0.033, then decrease at x = 0.066 and further increases with Co doping. The ε present in nanoparticles prepared by non-aqueous is smaller as compared to samples synthesized by sol gel method.

Table 9. Crystallite size (*D*), d-spacing (*d*), lattice constant (*a*) and strain (ε).

***x* (Co doping)**	***D* (nm)**	***d* (Å)**	***a* (Å)**	**ε**
0.000	52.63	2.5233	8.3689	0.00204
0.033	53.21	2.5254	8.3759	0.00197
0.066	51.62	2.5239	8.3709	0.00218
0.132	53.10	2.5248	8.3739	0.00195
0.264	56.50	2.5254	8.3758	0.00191
0.528	59.38	2.5329	8.4008	0.00179

Morphology and stoichiometry studies: FESEM micrographs of prepared samples at x = 0, 0.132 and 0.528 are shown in fig.12. The FESEM micrographs show uniform grains distribution as compared to previous synthesized samples by sol-gel method. It is also found that samples prepared by non-aqueous method are highly crystalline in nature.

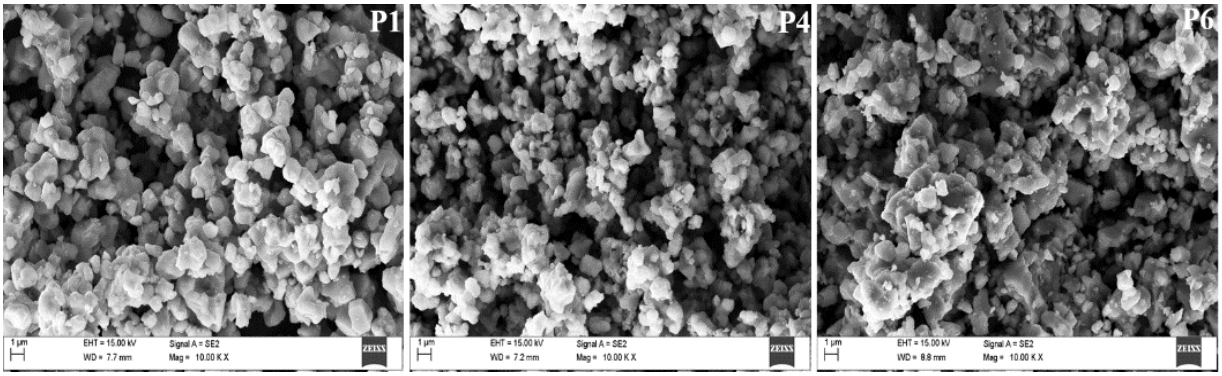

Fig.12: FESEM micrographs (P1) x = 0, (P4) x = 0.132 and (P6) x = 0.528.

The EDX spectra of $Ni_{0.6-x}Zn_{0.4}Co_xFe_2O_4$ nanoparticles at x = 0, 0.132 and 0.528 are being shown in fig.13. The atomic compositions of the samples are tabulated in table 10. The EDX results revealed that in prepared samples all elements are found in defined and expected ratio.

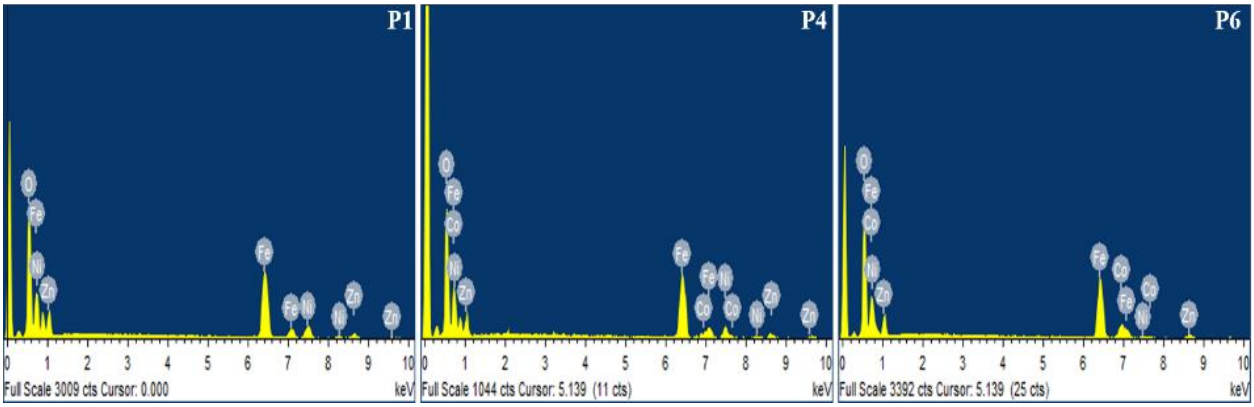

Fig.13: EDX spectra of $Ni_{0.6-x}Zn_{0.4}Co_xFe_2O_4$ (P1) x = 0, (P4) x = 0.132 and (P6) x = 0.528.

Table 10. Atomic percentage (At. %) of $Ni_{0.6-x}Zn_{0.4}Co_xFe_2O_4$ at x = 0, 0.132 and 0.528 obtained from EDX measurement.

Composition (x)	O (At. %)	Fe (At. %)	Ni (At. %)	Zn (At. %)	Co (At. %)
0	51.07	32.73	9.93	6.27	0
0.132	53.27	31.77	7.90	5.52	1.54
0.528	51.89	32.56	1.07	5.93	8.55

Magnetic studies: Fig.14 shows the M-H curve of prepared samples. The value of saturation magnetization (M_s), magnetic moment (M_μ) retentivity (M_r), coercivity (H_c), Squareness ratio (M_r/M_s) and magneto crystalline anisotropy energy (K) are presented in table 11.

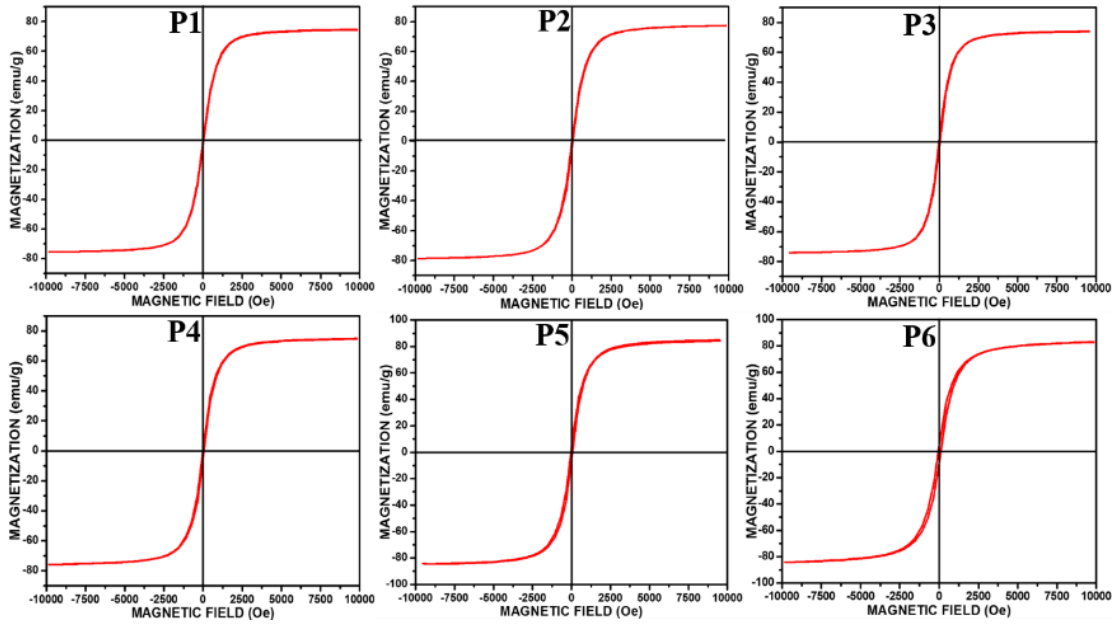

Fig.14: Hysteresis loops of $Ni_{0.6-x}Zn_{0.4}Co_xFe_2O_4$ (P1) x = 0, (P2) x = 0.033, (P3) x = 0.066, (P4) x = 0.132, (P5) x = 0.264 and (P6) x = 0.528 at room temperature (300K).

The M_s value of prepared nanoparticles prepared by non-aqueous method is higher than that of sample prepared by sol-gel method (objective 2.2). The value of M_r and H_c continuously increase with Co doping. The H_c value of samples prepared by non-aqueous method is smaller than samples synthesized by sol-gel method (objective 2.2).

Table 11. Saturation magnetization (M_s), magnetic moment (M_μ), retentivity (M_r), coercivity (H_c), squareness ratio (M_r/M_s) and magneto crystalline anisotropy (K) measured from VSM.

x (Co Doping)	D (nm)	M_s (emu/g)	M_μ (μ_B)	M_r (emu/g)	H_c (Oe)	M_r/M_s	K (erg/cm^3
0.000	52.63	75.17	3.190	1.23	21.04	0.0163	790.78
0.033	53.21	77.85	3.304	2.24	27.97	0.0287	1088.73
0.066	51.62	73.94	3.138	2.70	31.28	0.0365	1156.42
0.132	53.10	75.07	3.186	3.67	42.90	0.0488	1610.25
0.264	56.50	84.42	3.584	5.64	59.90	0.0668	2528.37
0.528	59.38	83.72	3.555	7.48	88.78	0.0893	3716.33

Theoretical structural and magnetic analysis: The proposed cations distribution, theoretically calculated lattice constant (a_{th}), mean ionic radii of tetrahedral (r_A) and octahedral (r_B) sites [12] and magnetic moment (N_μ) [13] are listed in table 12. The theoretically calculated a_{th} and N_μ follows the same trend as experimental a and M_μ values varies and support the proposed cations distributions.

Table 12. Proposed Cations distribution, r_A, r_B, $a_{th,}$ a and N_μ.

x	Cation Distribution Site A	Cation Distribution Site B	r_A (Å)	r_B (Å)	a_{th} (Å)	a (Å)	N_μ
0.000	$(Zn_{0.4}Fe_{0.6})$	$[Ni_{0.6}Fe_{1.4}]$	0.7300	0.6760	8.4786	8.3689	5.200
0.033	$(Zn_{0.4}Fe_{0.6})$	$[Ni_{0.567}Co_{0.033}Fe_{1.4}]$	0.7300	0.6769	8.4810	8.3759	5.233
0.066	$(Zn_{0.26}Co_{0.05}Fe_{0.69})$	$[Ni_{0.534}Zn_{0.14}Co_{0.016}Fe_{1.31}]$	0.7127	0.6864	8.4797	8.3709	4.066
0.132	$(Zn_{0.35}Co_{0.03}Fe_{0.62})$	$[Ni_{0.468}Zn_{0.05}Co_{0.102}Fe_{1.38}]$	0.7274	0.6822	8.4870	8.3739	4.952
0.264	$(Zn_{0.38}Co_{0.02}Fe_{0.6})$	$[Ni_{0.336}Zn_{0.02}Co_{0.244}Fe_{1.4}]$	0.7285	0.6840	8.4977	8.3758	5.344
0.528	$(Zn_{0.33}Co_{0.07}Fe_{0.6})$	$[Ni_{0.072}Zn_{0.07}Co_{0.458}Fe_{1.4}]$	0.7247	0.6931	8.5161	8.4008	5.308

Conclusion:

Structural as well as magnetic properties were investigated by XRD, FESEM, EDX and VSM. Single phase spinel cubic structure nanoparticles with stoichiometry were prepared by sol-gel method annealed at high temperature 1100^{o}C. The enhancement in saturation magnetization has been observed in terms of distribution of Co^{2+} ions in octahedral sites with doping when samples annealed at low temperature 700^{o}C. The reduction in saturation magnetization with doping at high annealing temperature 1100^{o}C is due to distribution of Co^{2+} ions in tetrahedral sites. Single

phase spinel cubic structure with homogeneous grains distribution, high crystalline and stoichiometric in nature nanoparticles has been successfully synthesized by non-aqueous method. The nanoparticles prepared by non-aqueous method has high saturation magnetization, low retentivity and low coercivity and can be used in target drug delivery, hyperthermia applications, EMI shielding and recording devices applications. Theoretically calculated lattice constant, Neel magnetic moment and other parameters calculated from proposed cations distribution have good agreement with results that obtained from experimental data. Moreover, non-aqueous method is very simple, cost effective, low temperature synthesis process and nanoparticles can be prepared in short duration with multicomponent system.

4. References:

1. A. C. F. M. Costa., *et. al.* Journal of magnetism and magnetic materials 256, 174 (2003).
2. J. B. D. Silva., *et. al.* Journal of magnetism and magnetic materials 226, 1393 (2001)
3. M. Jalaly., *et. al.* Journal of Alloys and Compound 480, 737 (2009).
4. M. Sertkol., *et. al.* Journal of Magnetism and Magnetic Materials 321, 157 (2009).
5. P. G. Bercoff., *et. al.* Journal of Magnetism and Magnetic Materials 213, 56 (2000).
6. S. R. Shannigrahi., *et. al.* Journal of Magnetism and Magnetic Materials 324, 140 (2012).
7. S. Thakur., *et. al.* Journal of Physical Chemistry C 113, 20785 (2009).
8. M. Sivakumar., *et. al.* Journal of Physical Chemistry B 110, 15234 (2006).
9. R. Kumar., *et. al.* Journal of Superconductivity and Novel Magnetism 28, 3557 (2015).
10. M. A. Iqbal., *et. al.* Journal of Alloys and Compounds 579, 181 (2013).
11. S. Thakur., *et. al.* Journal of Magnetism and Magnetic Materials 321, 1 (2009).
12. R. Sharma., *et. al.* Journal of Alloys and Compounds 684, 569 (2016).
13. D. Venkatesh., *et. al.* Journal of Magnetics 20, 229 (2015).
14. S. Chakrabarty., *et. al.* Journal of Alloys and Compounds 625, 216 (2015).

5. Publications:

1. Rajinder Kumar, Hitanshu Kumar, Manoj Kumar, Ragini Raj Singh, and P. B. Barman. "Enhanced Saturation Magnetization in Cobalt Doped Ni-Zn Ferrite Nanoparticles." ***Journal of Superconductivity and Novel Magnetism*** 28, no. 12 (2015): 3557-3564.

2. Rajinder Kumar, Hitanshu Kumar, Ragini Raj Singh, and P. B. Barman. "Variation in magnetic and structural properties of Co-doped Ni–Zn ferrite nanoparticles: a different aspect." ***Journal of Sol-Gel Science and Technology*** 78, no. 3 (2016): 566-575.

3. Rajinder Kumar, Ragini Raj Singh, and P. B. Barman. "Cobalt Doped Nickel Zinc Ferrite nanoparticles–Xrd Analyses an Insight". **International Journal of Scientific & Engineering Research** 5 (5) 2014.

Conference publication:

1. Rajinder Kumar, Hitanshu Kumar, Ragini Raj Singh, and P. B. Barman. "Structural analysis of emerging ferrite: Doped nickel zinc ferrite." In *ADVANCED MATERIALS AND RADIATION PHYSICS (AMRP-2015): 4th National Conference on Advanced Materials and Radiation Physics*, vol. 1675, p. 030003. **AIP Publishing**, 2015.

Communicated:

1. Deviation in Structural and Magnetic Properties due to Cations Distribution and Spin Canting Effect: Experimental and Theoretical Verification.

2. Development of Co doped Ni-Zn ferrite nanoparticles by Non-Aqueous method and their structural and magnetic studies.